**Proceedings of the ASME 2021**
**International Design Engineering Technical Conferences and**
**Computers and Information in Engineering Conference**
**IDETC/CIE 2021**
**August 17-20, 2021, Virtual, Online**

# IDETC2021-67865

# APPROXIMATING HINGES WITH MULTIMATERIAL COMPLIANT JOINTS

**Independence Talken**
College of Law
University of Nebraska
Lincoln, Nebraska 68583
Email: italken@alumni.nd.edu

**Zijuan Liang**
Department or Aerospace &
Mechanical Engineering
University of Notre Dame
Notre Dame, Indiana 46556
Email: zliang3@nd.edu

**Mark Plecnik***
Department or Aerospace &
Mechanical Engineering
University of Notre Dame
Notre Dame, Indiana 46556
Email: plecnikmark@nd.edu

## ABSTRACT

*This paper investigates the use of multimaterial compliant joints produced through additive manufacturing in order to approximate a revolute joint. Compliant joints benefit from low friction and reduced wear, but at the cost of increased joint stiffness, reduced range of motion, and a reduced ability to resist loading. In addition, they might also provide a poor approximation of the revolute joints they intend to replace. In this paper, we experiment with three multimaterial compliant joint configurations. The first joint emphasizes accurate kinematics, the second joint aims to reduce axis-aligned stiffness, and the third joint compromises between the two. Samples were fabricated on a desktop 3D printer using PLA (polylactic acid) as the rigid material and TPU (thermoplastic polyurethane) for its flexibility. Samples were measured for tensile stiffness, torsional stiffness, range of motion, and approximation of a hinge motion. Our results indicate design trade offs where joints that measure most ideal for one property will be least ideal for another. The most novel design in this paper straddles this trade off. In the end, the suitability of each joint design is determined by the loading, accuracy, and range of motion requirements posed by a given application.*

*Address all correspondence to this author.

## 1 INTRODUCTION

Compliant flexure hinges provide a range of benefits versus traditional pin and bearing revolute joints, including weight savings, ease of manufacture, the removal of friction, good wear properties, and eliminating the assembly of multiple parts. However, this comes at a cost. Pin and bearing joints are capable of resisting large loads and provide continuous rotation. The use of flexures introduces a limited range of motion and a new angle dependent stiffness. Furthermore, if the intent is to replace traditional hinges, flexures less accurately approximate rotations.

Single material joints are particularly challenged in high load applications. By choosing a single material, both rigid and flexible sections incorporate the same elastic modulus, leading thin necks at flexures susceptible to fracture. With two materials, elastic moduli could be mixed in a conventional way using a flexible material to form a joint that connects two rigid halves. However, there may exist less straightforward geometries that address some of the aforementioned weaknesses. We explore this possibility here.

Multimaterial additive manufacturing is accessible today through many commercial 3D printers. Despite this manufacturing capability, the geometrical space of multimaterial compliant joint designs remains largely unexplored. In this paper, we evaluate three joint geometries according to the usual weaknesses of compliant joints. In particular, we focus on resistance to tensile loads, reducing axis-aligned torsional stiffness, range of motion, and the ability to approximate rotation. The designs evaluated are

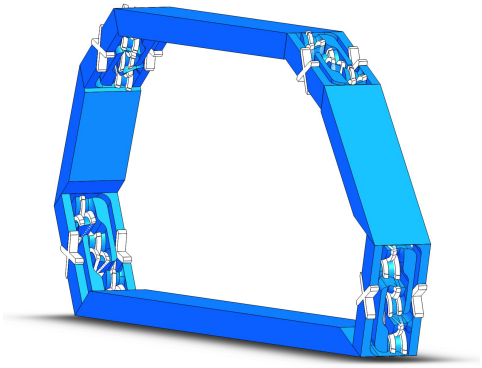

**FIGURE 1**. A four bar mechanism designed with multimaterial joints.

printed from rigid PLA filament and flexible TPU filament. They include two rigid links connected by a single X-shaped section of TPU, rounded rigid links connected by TPU straps that approximate an epicyclic motion, and a more novel combination of these two joint designs. A four-bar linkage constructed from this combination joint is depicted in Fig. 1.

In the rest of the paper, we review relevant literature in Section 2 and introduce the evaluated joint designs in Section 3. Section 4 describes fabrication measurement methods and Section 5 offers a discussion of results.

## 2 LITERATURE

Weisbord and Paros [1] presented an early analysis of a few classic flexure designs. More recently Trease, Moon, and Kota [2] presented a catalog of improved flexure joint designs and their analytical stiffness equations. Their work addressed range of motion, axis drift, off-axis stiffness, and reduced stress concentrations in single material compliant joints. Choi, Sreenivasan, and Choi [3] demonstrated how to use flexure joints to design a large displacement XY stage for usage in a semiconductor application. Xu, Dai, and Zhou [4] studied the design of notch flexures, presenting analytic models for elliptic, circular, parabolic, and hyperbolic shaped notches. They propose comparing flexure designs by a "hinge index," the ratio of rotational precision over rotational stiffness. Yong, Fu, and Handley [5] presented a review of stiffness model equations for the circular notch, comparing these models to FEA results. McInroy and Hamann [6] designed three hexapod positioners that incorporate flexures, and showed how to implement position, velocity, acceleration, and force control for their flexure-based mechanisms. Naves et al. [7] designed a flexure-based suspension for high torque motors. Goldfarb and Speich [8] present a more unique flexure hinge design called a split-tube flexure. This design achieves its primary mode of compliance by twisting a thin-walled open-section member. Their approach increased stiffness along structural axes.

Peraza-Hernandez et al. [9] provide a review of origami-inspired active mechanisms, covering devices that incorporate dissimilar materials to enable self-folding. A number of small scale robot designs have implemented sandwiched structures of flexible polymer films and rigid plates (cardstock or composite) for both flapping and legged locomotion [10, 11]. Bejgerowski et al. [12, 13] used multimaterial injection molding in the construction of a micro air vehicle. Vogtmann, Gupta, and Bergbreiter [14] laser cut rigid links that were refilled at joint locations with elastomeric material to fabricate leg mechanisms for millirobots. Bruyas et al. [15] designed a multimaterial compliant joint of a helical shape printed by a Polyjet 3D printer. Jeanneau et al. [16] demonstrated the use of compliant joints that exhibit an epicyclic rolling motion, and used them in the fabrication of a three degree-of-freedom manipulator. Halverson, Howell, and Magleby [17] designed a similar joint, using Kevlar straps to connect rigid members. They performed fatigue testing and demonstrated functionality beyond 100,000 cycles.

In this work, we evaluate three multimaterial joint designs, all fabricated from a 3D printer. These designs include (1) two rigid links of PLA connected by an X-shaped section of TPU, (2) epicyclic rolling contact joints, and (3) a combination joint. Joint designs were fabricated and measured to assess their resistance to tensile loading, mitigation of axis-aligned torsional stiffness, range of motion, and approximation of a pivot.

## 3 CONFIGURATIONS

This paper considers three major joint designs that we call the *XfleX*, *Ivy*, and *Xepi* joints. Each joint consists of rigid links, printed out of PLA, and flexible connections, printed out of TPU.

### XfleX

The XfleX joint (Fig. 2a) combines two rigid PLA members with a flexible X section of TPU in the middle. So that the joint's strength is not limited by the bond between PLA and TPU, columns of TPU are place on the sides of the X and pass through holes in the rigid links to form interlocked geometry.

### Ivy

The Ivy joint (Fig. 2b) consists of two rigid PLA links with semicircle ends that roll on each other, producing an epicyclic motion. The PLA links are connected by TPU straps that wrap around the semicircular surfaces. Straps are held in place by interlocking into PLA so as to not depend on a bond between these dissimilar materials. Seeing that the resulting motion is epicyclic, the center of rotation moves considerably as the joint rotates. The strength of this joint is in its compressive stiffness. Stiffness in all other directions is compromised by the flexbility of the TPU straps.

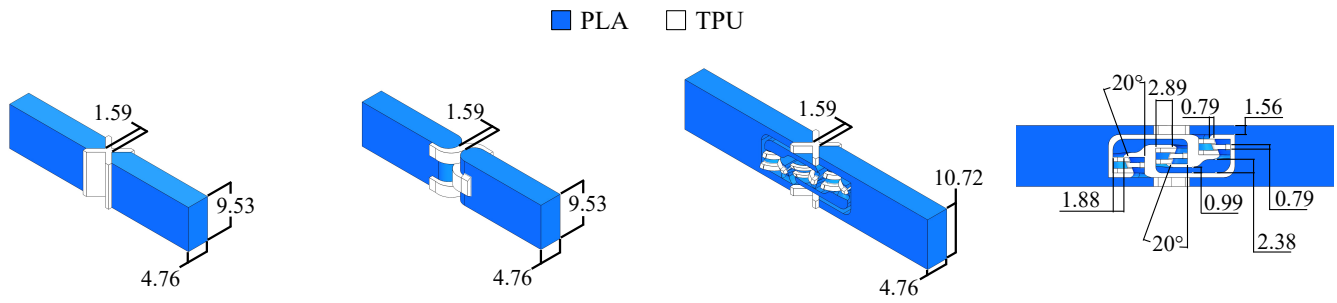


**FIGURE 2**. The joint configurations tested in this paper include (a) the XfleX joint, (b) the Ivy joint, (c) and the Xepi joint. (d) An additional view of the Xepi joint. Dimensions in mm.

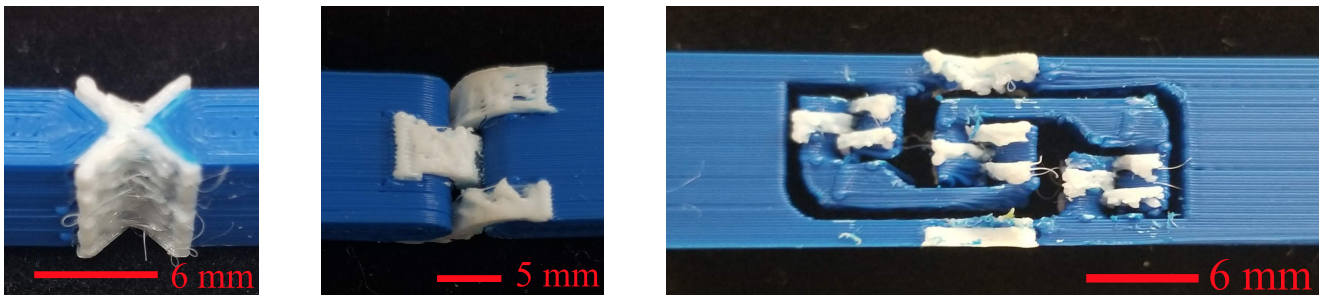


**FIGURE 3**. Print quality results for (a) the XfleX joint, (b) the Ivy joint, and (c) the Xepi joint.

### Xepi

The Xepi joint (Fig. 2c) is a combination of the XfleX and Ivy joints. It comprises of two XfleX joints on its sides, and three conical derivations of Ivy joints along its center, see Fig. 2d. The role of the XfleX joints is to geometrically constrain relative motion between the two halves to a near rotation. The arrangement of Ivy joints were positioned to transform this joint's natural compressive stiffness into tensile stiffness in the combination joint. When the overall joint is in tension, each Ivy joint is in compression. Three Ivy joints were included in order to increase the degrees-of-freedom of this subchain so as to not geometrically overconstrain the Xepi joint. Specifically, if only a single Ivy joint were included, its epicyclic motion would have to fight the rotation of the XfleX joint. Conical surfaces were chosen so that Ivy modules interlock with each other when the whole joint is in tension. This modification was made after earlier versions were observed to bend and slip past each other when straight semicircles were used.

## 4 METHODS

Test samples were printed and were measured for torsional stiffness along the joint axis, tensile stiffness, range of motion, and deviation from a pure rotation. The testing sequence followed the ordering of motion tracking, torsional testing, and then tensile testing. Three samples of each joint underwent this sequence.

### Fabrication

The multimaterial compliant joints were printed with PRO Series Tough PLA and NinjaFlex TPU. All samples were printed with a BCN3D Sigmax, which features dual extruders to accommodate each material. TPU was printed at 225°F with 100% infill, while the PLA was printed at 215°F with 20% infill. A 0.4 mm nozzle was used for both materials. Fig. 3 displays the resulting print quality. Irregularities mainly formed in the TPU sections. Features were printed to be as small as possible while not compromising functionality.

### Motion Tracking

Motion tracking was used to measure both range of motion and deviation from a true pivot. None of the joints in this work are capable of continuous rotation. Each joint possesses a limited range of motion, and so should only be utilized when relative rotation requirements fall within their range. Linkage mechanisms often possess joints that oscillate through small relative rotations.

Each sample's deviation from a true pivot was measured by

tracking its instantaneous center. For a traditional pin joint, the instantaneous center stays fixed on the center of the pin. Deviations from this center are possible through joint slop or material deflection. The composite joints of this paper all deviate from a true pivot, due to their various geometric configurations. A smaller pivot deviation is more desirable because it approximates the motion of a revolute pin joint. We seek this characteristic because many existing modelling techniques, mechanism designs, and design methods are based on the use of revolute joints to approximate the constraint of a circle.

Motion tracking was recorded by a camera placed 27 cm above each sample's approximate axis of rotation. Samples were fixed at one end, and their free end was rotated to their limit. Markings were placed on joints to aid in video processing of motion capture software: two on the fixed link, two on the moving link, and one on the joint's center when in its aligned configuration, see Fig. 4. Tracker Video Analysis software was used to analyze and extract position information for each of the five marks.

Data was smoothed using a moving average with a window of five video frames. The two marks on the fixed link served to establish its reference frame. The motions of the remaining marks were kinematically inverted to this fixed frame. That is, with the origin of the fixed frame placed at the marker closer to the joint, called **f**, then the transformation that inverts the remaining points, i,e, the center mark **c**, and the marks on the moving link, $\mathbf{m}_A$ and $\mathbf{m}_B$, is

$$T(\mathbf{x}) := \begin{bmatrix} \cos\theta & -\sin\theta \\ \sin\theta & \cos\theta \end{bmatrix}^T \left(\mathbf{x} - \mathbf{f}\right) \quad \text{for} \quad \mathbf{x} = \mathbf{c},\ \mathbf{m}_A,\ \mathbf{m}_B \qquad (1)$$

where $\theta$ is the angle of the "fixed" link, which jiggles during data collection. Eq. (1) removes this jiggle.

The relative angle is named $\phi$, and the transformed marker positions are named $\hat{\mathbf{C}}$, $\hat{\mathbf{m}}_A$, and $\hat{\mathbf{m}}_B$. The position of the joint's center in the first frame (when the link is aligned) is named $\hat{\mathbf{c}}_0$. This point can be transformed to follow along in the moving frame defined by $\hat{\mathbf{m}}_A$ and $\hat{\mathbf{m}}_B$. The relevant transformation is

$$\hat{\mathbf{C}} = \begin{bmatrix} \cos(\phi-\phi_0) & -\sin(\phi-\phi_0) \\ \sin(\phi-\phi_0) & \cos(\phi-\phi_0) \end{bmatrix}^T \left(\hat{\mathbf{c}}_0 - \hat{\mathbf{m}}_{A0}\right) + \hat{\mathbf{m}}_A \qquad (2)$$

The zero subscript is used to denote points in the first frame.

Equation (2) may be applied to all video frames to track the motion of $\hat{\mathbf{C}}$ throughout the joint's rotation. An example of the path of $\hat{\mathbf{C}}$ for the Ivy joint is shown in Fig. 4. We term the distance of the deviated center from its start position as the *pivot deviation*. Naming pivot deviation as $\delta$, its definition is

$$\delta = |\hat{\mathbf{C}} - \hat{\mathbf{c}}_0| \qquad (3)$$

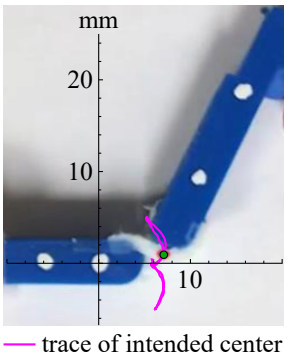


**FIGURE 4**. Motion tracking of an Ivy joint. The trace of the instantaneous center is displayed. Marks were added to the sample to aid in video processing.

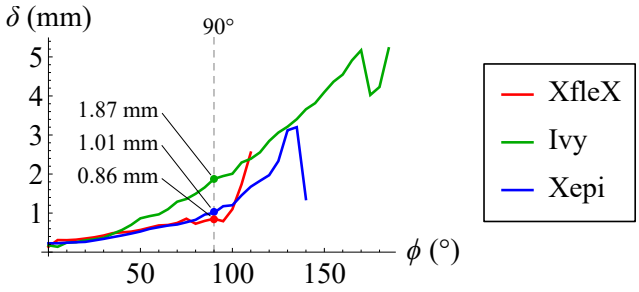


**FIGURE 5**. The average of pivot deviation plotted against rotation angle for each joint design. XfleX demonstrates the least amount of deviation from a true pivot.

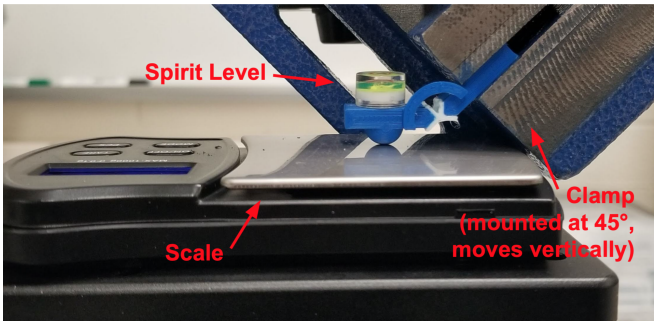


**FIGURE 6**. The torque required to deflect an XfleX sample to 45° is measured.

The average of pivot deviation plotted against rotation angle for each joint design is shown in Fig. 5. This plot was obtained by measuring three samples of each joint type rotated in both directions. The aligned configuration corresponds to 0°. Data for the plot was assembled for each joint type by averaging over all samples and in both rotation directions. In order to compare designs against each other, we take deviation of $\hat{\mathbf{C}}$ at 90°.

### Torsional Stiffness

Torsion testing was performed in order to determine the torsional stiffness of each joint as it bends along the intended axis. A lower torsional stiffness is desirable because it requires less driving torque. Fig. 6 illustrates the XfleX undergoing a torsion test. A suspended clamp holds one arm of the joint at 45° while the other arm is balanced on a scale. Samples were printed with a hemisphere at one end of the joint to provide a point contact between the joint and the scale. This ensured that the moment arm was measured from the center of the ball to the center of the joint. A miniature spirit level indicated the inclination of the scale arm. The clamp, which can only move in the vertical direction, is lowered until the spirit level indicated the scale arm was horizontal. Torsional stiffness is recorded as the scale readout times gravity times the moment arm divided by the rotation angle of 45°.

### Tensile Stiffness

Tensile stiffness measures a joint's resistance to deflection under loading. Unintended deflections negatively impact the accuracy of a mechanism. Multimaterial composite joints are particularly susceptible to tensile loads as the flexible TPU easily stretches. The inner rolling surfaces of the Xepi joint were designed with this weakness in mind. Tensile testing was performed on a universal testing machine (Admet eXpert 7603). A picture of a Xepi sample pulled in tension on the machine is shown in Fig. 7. The machine was programmed to move upward at $0.5\frac{\text{mm}}{\text{s}}$ over a distance of 3 mm. Force and displacement data were collected. Tensile stiffness was calculated by considering thee force generated at 0.5 mm of deflection to the undeflected sample, see Fig. 8.

## 5 RESULTS

A compilation of measurements obtained in this paper appears in Fig. 9. Each joint configuration is characterized by a mix of strengths and weaknesses across performance metrics. Fig. 9 compares designs according to tensile stiffness, torsional stiffness, pivot deviation, and range of motion. Each bar is labelled with the measurement of each corresponding property. The numbered horizontal axis indicates performance relative to the best performer with respect to that property. For example, the XfleX design exhibited the greatest tensile stiffness at 68.7 N/mm. The relative performance of the Ivy and Xepi designs with respect to tensile stiffness are 6.9/68.7 = 10% and 26.2/68.7 = 38%, respectively. As an additional example, the Ivy design exhibited the best (lowest) torsional stiffness with a value of 3.5 Nmm/rad. The relative performance of XfleX and Xepi designs was then computed as 3.5/18.6 = 19% and 3.5/7.8 = 45%, respectively.

The XfleX configuration was the stiffest in tension and demonstrated the least amount of deviation from a true pivot.

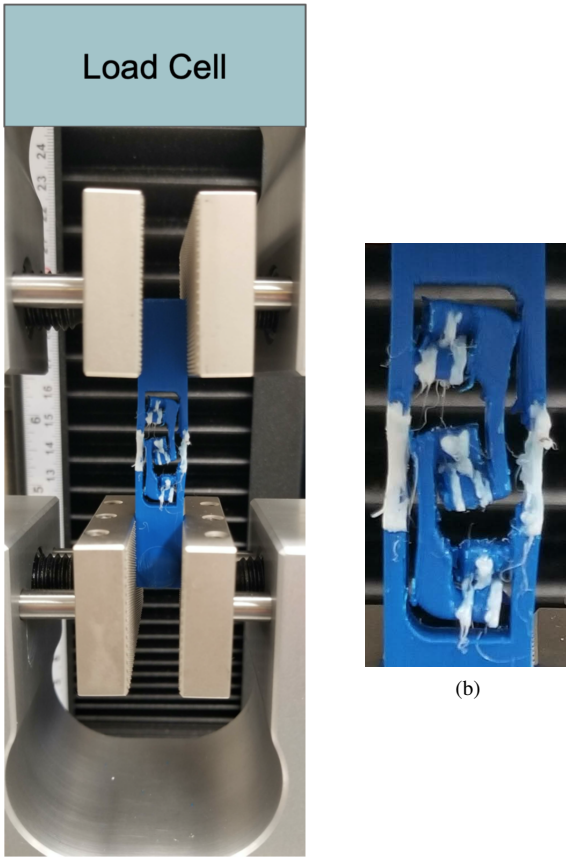


(a) (b)

**FIGURE 7**. (a) A Xepi joint sample clamped in the universal testing machine and under 38 N of tensile load. (b) A close-up of Xepi joint features under tensile load.

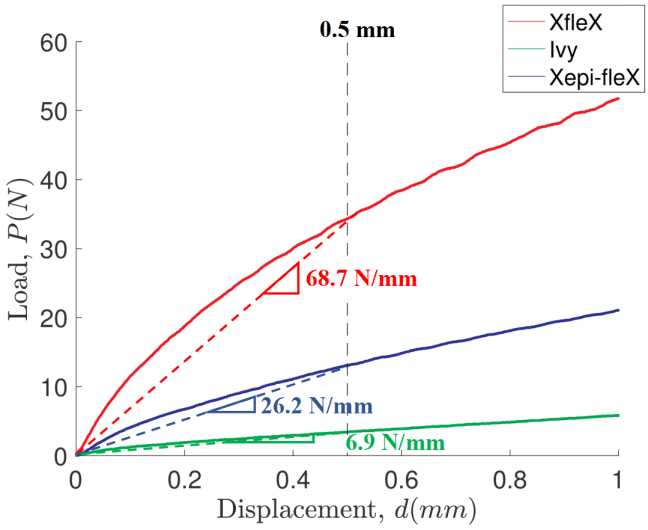


**FIGURE 8**. Tensile load vs. axial deflection for each joint design. XfleX exhibited the greatest tensile stiffness.

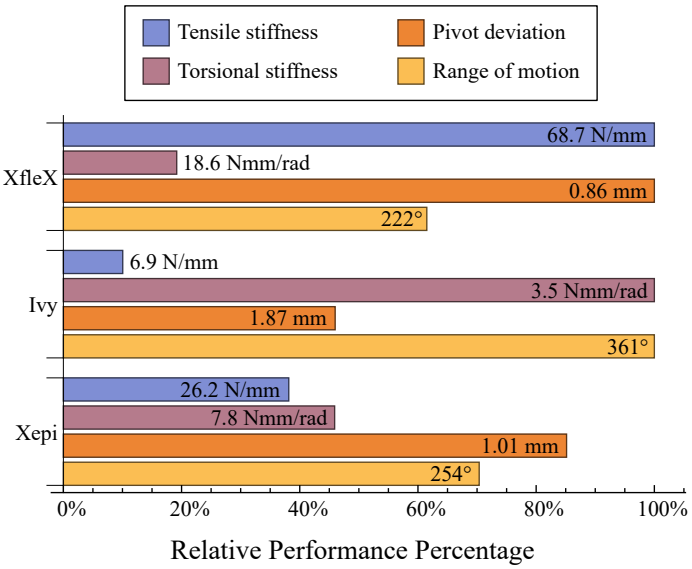


**FIGURE 9**. Comparison of tensile stiffness, torsional stiffness, pivot deviation, and range of motion for each joint type.

Given its resistance to deflection, XfleX would be a good choice when high loads are present. Its low pivot deviation suggests this joint to be a good choice in applications where more position accuracy is needed. Its weakness is that it exhibited high torsional stiffness. A mechanism constructed of many of these joints would require greater torques to drive.

The lowest values of torsional stiffness were measured in the Ivy joint. A mechanism constructed of these joints could be driven by lower torques. The trade off of this is that the Ivy joint exhibited the least tensile stiffness, making this design less than ideal for high loading situations. In addition, the Ivy joint exhibited the least accurate approximation of a pivot. However, its epicyclic motion allows it to rotate further than the other joints. The Ivy joint would be most suitable for applications that demand a large range of motion and where low driving torques are important.

The Xepi joint measured as the moderate choice for all properties. It was neither the best or worse performer for each measured property. Its interlocking inner mechanism allows it to withstand tensile loads with less deflection than the Ivy design. The addition of two X-shaped sections of TPU at its core constrains its motion to limit deviation from a true pivot. In terms of range of motion, it performed similar to the XfleX configuration.

## 6 CONCLUSION

By mixing materials of different stiffnesses, joint geometries are not limited to thin flexures susceptible to bending stress and fatigue. Furthermore, 3D printing multimaterial joints allows the explroation of a variety of geometries. In this paper, we investigate three different multimaterial joint configurations, named XfleX, Ivy, and Xepi. All joints are printed from PLA and TPU. The XfleX design consists of a single core section of TPU in the shape of an X. The Ivy joint consists of two half cylinders that roll in an epicyclic motion as connected by straps of TPU. Finally, the Xepi joint is a combination of the XfleX and Ivy designs. It possesses three interlocking rolling joints as an inner mechanism bounded by two TPU X's on its sides. The inner mechanism is arranged so that when the joint is in tension, all rolling surfaces are in compression. In this way, PLA surfaces push against each other rather than TPU sections stretching. Furthermore, the Xepi joint's rolling surfaces actually consist of interlocking conic surfaces rather than cylinders. This is in order to promote interlocking of the inner mechanism during tensile loading. Motion tracking, torsion, and tensile testing was executed in order to assess each configuration's performance. From motion recordings, a joint's range of motion was measured as well as its approximation of a pivot. Torsional and tensile stiffness testing was also performed. The results indicated the XfleX design to be the most ideal in terms of tensile stiffness as well as providing the best approximation of a pivot. However, it exhibited high torsional stiffness. The Ivy design exhibited the largest angular range of motion, but its tensile stiffness values were less ideal. The Xepi design fell in between the XfleX and Ivy designs for all measured properties. Each of the designs presented in this paper are warranted based on the loading, accuracy, and range of motion requirements for a given application.

## ACKNOWLEDGMENT

The authors gratefully acknowledge the support of the National Science Foundation Award No. CMMI-2041789.

## REFERENCES

[1] Weisbord, L., and Paros, J. M., 1965. "How to Design Flexure Hinges". *Machine Design,* ***27***(3), pp. 151–157.

[2] Trease, B. P., Moon, Y.-M., and Kota, S., 2005. "Design of Large-Displacement Compliant Joints". *Journal of Mechanical Design,* ***127***(4), July, pp. 788–798.

[3] Choi, Y.-J., Sreenivasan, S. V., and Choi, B. J., 2008. "Kinematic design of large displacement precision XY positioning stage by using cross strip flexure joints and over-constrained mechanism". *Mechanism and Machine Theory,* ***43***(6), June, pp. 724–737.

[4] Xu, N., Dai, M., and Zhou, X., 2017. "Analysis and Design of Symmetric Notch Flexure Hinges". *Advances in Mechanical Engineering,* ***9***(11), pp. 1–12.

[5] Yong, Y. K., Lu, T.-F., and Handley, D. C., 2008. "Review of circular flexure hinge design equations and derivation of empirical formulations". *Precision Engineering,* ***32***(2), Apr., pp. 63–70.

[6] McInroy, J., and Hamann, J., 2000. "Design and control of flexure jointed hexapods". *IEEE Transactions on Robotics and Automation,* ***16***(4), Aug., pp. 372–381.
[7] Naves, M., Nijenhuis, M., Hakvoort, W. B. J., and Brouwer, D. M., 2020. "Flexure-based 60 degrees stroke actuator suspension for a high torque iron core motor". *Precision Engineering,* ***63***, May, pp. 105–114.
[8] Goldfarb, M., and Speich, J. E., 1999. "A Well-Behaved Revolute Flexure Joint for Compliant Mechanism Design". *Journal of Mechanical Design,* ***121***(3), Sept., pp. 424–429.
[9] Peraza-Hernandez, E. A., Hartl, D. J., Jr, R. J. M., and Lagoudas, D. C., 2014. "Origami-inspired active structures: A synthesis and review". *Smart Materials and Structures,* ***23***(9), Aug., p. 094001.
[10] Hoover, A. M., and Fearing, R. S., 2008. "Fast scale prototyping for folded millirobots". In 2008 IEEE International Conference on Robotics and Automation, pp. 886–892.
[11] Wood, R. J., Avadhanula, S., Sahai, R., Steltz, E., and Fearing, R. S., 2008. "Microrobot Design Using Fiber Reinforced Composites". *Journal of Mechanical Design,* ***130***(5), May.
[12] Bejgerowski, W., Gerdes, J. W., Gupta, S. K., and Bruck, H. A., 2011. "Design and fabrication of miniature compliant hinges for multi-material compliant mechanisms". *International Journal of Advanced Manufacturing Technology,* ***57***, pp. 437–452.
[13] Bejgerowski, W., Gerdes, J. W., Gupta, S. K., Bruck, H. A., and Wilkerson, S., 2011. "Design and Fabrication of a Multi-Material Compliant Flapping Wing Drive Mechanism for Miniature Air Vehicles". In ASME 2010 International Design Engineering Technical Conferences and Computers and Information in Engineering Conference, American Society of Mechanical Engineers Digital Collection, pp. 69–80.
[14] Vogtmann, D. E., Gupta, S. K., and Bergbreiter, S., 2011. "Multi-material compliant mechanisms for mobile millirobots". In 2011 IEEE International Conference on Robotics and Automation, pp. 3169–3174.
[15] Bruyas, A., Geiskopf, F., Meylheuc, L., and Renaud, P., 2014. "Combining Multi-Material Rapid Prototyping and Pseudo-Rigid Body Modeling for a new compliant mechanism". In 2014 IEEE International Conference on Robotics and Automation (ICRA), pp. 3390–3396.
[16] Jeanneau, A., Herder, J., Laliberté, T., and Gosselin, C., 2008. "A Compliant Rolling Contact Joint and Its Application in a 3-DOF Planar Parallel Mechanism With Kinematic Analysis". In ASME 2004 IDETC/CIE, pp. 689–698.
[17] Halverson, P. A., Howell, L. L., and Magleby, S. P., 2010. "Tension-based multi-stable compliant rolling-contact elements". *Mechanism and Machine Theory,* ***45***(2), Feb., pp. 147–156.